# A Novel Transforming Growth Factor Beta-Induced Long Noncoding RNA Promotes an Inflammatory Microenvironment in Human Intrahepatic Cholangiocarcinoma

Aude Merdrignac,[1] Gaëlle Angenard,[1] Coralie Allain,[1] Kilian Petitjean,[1] Damien Bergeat,[1] Pascale Bellaud,[1] Allain Fautrel,[1] Bruno Turlin,[1] Bruno Clément,[1] Steven Dooley,[2] Laurent Sulpice,[1] Karim Boudjema,[1] and Cédric Coulouarn[1]

**Intrahepatic cholangiocarcinoma (iCCA) is a deadly liver primary cancer associated with poor prognosis and limited therapeutic opportunities. Active transforming growth factor beta (TGF$\beta$) signaling is a hallmark of the iCCA microenvironment. However, the impact of TGF$\beta$ on the transcriptome of iCCA tumor cells has been poorly investigated. Here, we have identified a specific TGF$\beta$ signature of genes commonly deregulated in iCCA cell lines, namely HuCCT1 and Huh28. Novel coding and noncoding TGF$\beta$ targets were identified, including a TGF$\beta$-induced long noncoding RNA (TLINC), formerly known as cancer susceptibility candidate 15 (CASC15). TLINC is a general target induced by TGF$\beta$ in hepatic and nonhepatic cell types. In iCCA cell lines, the expression of a long and short TLINC isoform was associated with an epithelial or mesenchymal phenotype, respectively. Both isoforms were detected in the nucleus and cytoplasm. The long isoform of TLINC was associated with a migratory phenotype in iCCA cell lines and with the induction of proinflammatory cytokines, including interleukin 8, both *in vitro* and in resected human iCCA. TLINC was also identified as a tumor marker expressed in both epithelial and stroma cells. In nontumor livers, TLINC was only expressed in specific portal areas with signs of ductular reaction and inflammation. Finally, we provide experimental evidence of circular isoforms of TLINC, both in iCCA cells treated with TGF$\beta$ and in resected human iCCA. *Conclusion*: We identify a novel TGF$\beta$-induced long noncoding RNA up-regulated in human iCCA and associated with an inflammatory microenvironment. (*Hepatology Communications* 2018;2:254-269)**

## Introduction

Cholangiocarcinomas (CCAs) comprise heterogeneous hepatobiliary tumors with cholangiocyte differentiation features. CCAs are classified as intrahepatic (iCCA), perihilar, and distal, based on their anatomic location.[1,2] In the liver, iCCA accounts for 5%-10% of all malignant primary cancers and ranks second after hepatocellular carcinoma (HCC). Importantly, both incidence and mortality rates of iCCA have increased significantly worldwide during the past decades.[2] To date, surgery is the best potentially curative treatment for iCCA but is feasible in less than 40% of cases. For these

*Abbreviations: CASC15, cancer susceptibility candidate 15; CCA, cholangiocarcinoma; circRNA, circular RNA; EMT, epithelial to mesenchymal transition; GSEA, gene set enrichment analysis; HCC, hepatocellular carcinoma; iCCA, intrahepatic cholangiocarcinoma; IL8, interleukin 8; ISH, in situ hybridization; LCM, laser capture microdissection; lncRNA, long non coding RNA; miRNA, miR, micro RNA; Q-RT-PCR, quantitative reverse-transcription polymerase chain reaction; RNase, ribonuclease; SMAD, SMAD family member; SNAI1, snail family transcriptional repressor 1; TGFβ, transforming growth factor beta; TLINC, transforming growth factor beta-induced long noncoding RNA; TLINC-L, long TLINC isoform; TLINC-S, short TLINC isoform.*

*Received November 1, 2017; accepted December 8, 2017.*

*Additional Supporting Information may be found at onlinelibrary.wiley.com/doi/10.1002/hep4.1142/full.*

*Supported by INSERM, University of Rennes 1, Institut National du Cancer (INCa, Cancéropôles Ile-de-France and Grand-Ouest), Ligue contre le cancer (cd35, cd44, cd49), Novartis Oncology, and Association Française pour l'Etude du Foie, France (to L.S., C.C.); and by Deutsche Forschungsgemeinschaft DFG DO373/13-1 (to S.D.).*

resectable early stage iCCAs, 5-year survival is about 40%. However, for unresectable advanced iCCA, the median survival is less than 15 months.[2] Although significant progress in understanding the molecular basis of iCCA pathogenesis has been achieved by high throughput strategies, including the identification of genetic, epigenetic, and genomic alterations (e.g., KRAS proto-oncogene guanosine triphosphatase [*KRAS*], isocitrate dehydrogenase 1/2 [*IDH1/2*] mutations, fibroblast growth factor receptor 2 [*FGFR2*] fusions), there is no approved molecular targeted therapy that significantly improves patient survival in iCCA.[1,3] Thus, iCCA remains characterized by limited therapeutic options and very poor prognosis.[1,3] One histologic feature of iCCA is the presence of a prominent desmoplastic stroma that is known to contribute to tumor onset and progression.[4,5] While previous studies largely focused on identifying molecular alterations in tumor cells, we recently characterized genomic alterations that occur in the tumor microenvironment of iCCA.[6] Thus, by combining laser microdissection and gene expression profiling, we demonstrated that the expression of transforming growth factor beta (TGF$\beta$) in the stroma of iCCA predicts a poor prognosis, suggesting that TGF$\beta$ may represent a potential therapeutic target in iCCA.[6]

TGF$\beta$ is a pleiotropic cytokine that controls fundamental cellular processes associated with carcinogenesis (e.g., proliferation, apoptosis, invasion, angiogenesis, immunity).[7] However, the actions of TGF$\beta$ in cancer are complex because TGF$\beta$ exhibits either tumor-suppressive or tumor-promoting properties, depending on the tumor stage. At an early stage, TGF$\beta$ exerts potent antiproliferative properties on precancerous epithelial cells, notably by inducing genes with cytostatic actions (e.g., cyclin-dependent kinase inhibitor 1A [*CDKN1A*]). At an advanced stage, cells become resistant to the cytostatic effects of TGF$\beta$, which then promotes tumor growth and metastatic progression, particularly as a potent inducer of epithelial–mesenchymal transition (EMT).[7,8] To date, the molecular mechanisms switching the TGF$\beta$ actions from tumor suppression toward tumor promotion are not fully understood and may depend on the cellular context.[9,10] Gene mutations in the canonical TGF$\beta$ signaling (e.g., SMAD family member 4 [*SMAD4*]) and crosstalk with proliferative pathways have been proposed to contribute to the loss of the tumor suppressor arm of TGF$\beta$ in several cancers.[9] In addition, recent evidence demonstrated that long noncoding RNA (lncRNA) could mediate the prometastatic properties of TGF$\beta$.[11,12] LncRNAs form a large and diverse class of long RNA molecules (>200 nucleotides) that do not encode proteins. LncRNAs emerged as key regulators involved in human carcinogenesis, including liver cancers.[13,14] Here, we characterized the transcriptional response of iCCA cell lines to TGF$\beta$ and identified novel TGF$\beta$-regulated genes, including a lncRNA that we named TGF$\beta$-induced lncRNA (*TLINC*, formerly known as *LINC00340* and cancer susceptibility candidate 15 [*CASC15*]). *TLINC* is induced by TGF$\beta$ in several settings, and the expression of specific isoforms correlates with an EMT phenotype. *TLINC* is strongly up-regulated in human



*View this article online at wileyonlinelibrary.com.*
*DOI 10.1002/hep4.1142*

*Potential conflict of interest: Nothing to report.*

## ARTICLE INFORMATION:

**From the [1]Institut National de la Santé et de la Recherche Médicale, INRA, Université de Rennes, CHU Rennes, UMR 1241, Nutrition Metabolisms and Cancer, Service de Chirurgie Hépatobiliaire et Digestive, Biosit, Biogenouest, Core Facility H2P2 and CRB Santé, Rennes, France; [2]Department of Medicine II, Medical Faculty Mannheim, Heidelberg University, Mannheim, Germany.**

## ADDRESS CORRESPONDENCE AND REPRINT REQUESTS TO:

**Cédric Coulouarn, Ph.D.**
**INSERM UMR 1241, CHU Pontchaillou**
**2 rue Henri Le Guilloux**
**F-35033 Rennes, France**
**E-mail: cedric.coulouarn@inserm.fr**
**Tel: +33-2-2323-3881**

iCCA and is associated with an enhanced expression of proinflammatory cytokines, including interleukin 8 (*IL8*). Finally, circular isoforms of *TLINC* are highlighted as promising biomarkers in patients with iCCA.

# Materials and Methods

## CELL CULTURE AND REAGENTS

HuCCT1 (RCB-1960) and Huh28 (RCB-1943) CCA cell lines were purchased at the RIKEN BioResource Center (Tsukuba-shi, Japan). Cells were grown in Roswell Park Memorial Institute 1640 medium (HuCCT1) or minimal essential medium (Huh28) supplemented with 100 U/mL penicillin, 100 $\mu$g/mL streptomycin, and 10% fetal bovine serum. HCC cell lines were purchased from ATCC and cultured as described.[15] LX2 cells were grown as described.[16] Freshly isolated human hepatocytes were purchased from Biopredic International (St. Grégoire, France). Cells were cultured at 37 °C in a 5% $CO_2$ atmosphere, and overnight serum starvation was performed before each treatment. Unless otherwise specified, cells were treated with 1 ng/mL recombinant human TGF$\beta$ (R&D Systems, Minneapolis, MN) and 10 µM TGF$\beta$ inhibitors (Sigma-Aldrich, St. Louis, MO).

## TGF$\beta$ SENSOR CELL LINES AND LUCIFERASE ACTIVITY

Stable TGF$\beta$ sensor cell lines were generated by using a pCignal Lenti-SMAD Reporter assay (Qiagen, Courtabeuf, France) according to the manufacturer's instructions. Briefly, cells were transduced with lentiviral particles (multiplicity of infection, 10; 8 µg/mL SureENTRY transduction reagent) and selected with 1 µg/mL puromycin for 5 days. Luciferase activity was determined with the Firefly Luciferase Assay System (Promega, Madison, WI) and normalized by the number of viable cells evaluated by a PrestoBlue cell viability reagent (Invitrogen, Carlsbad, CA).

## DNA TRANSFECTION

DNA constructs were kindly provided by Dr. Kristina A. Cole (Children's Hospital of Philadelphia, Philadelphia, PA) and Dr. Sumio Sugano (University of Tokyo, Tokyo, Japan). All constructs were amplified by transformation of One Shot TOP10 *Escherichia coli* (Invitrogen) and validated by DNA sequencing (Supporting Table S1) after DNA purification (Nucleobond Xtra plasmid maxiprep kit; Macherey Nagel, Hoerdt, France). DNA transfection was performed by using Lipofectamine 2000 (Invitrogen).

## PROTEIN ANALYSIS

A Quantikine enzyme-linked immunosorbent assay human TGF$\beta$1 immunoassay (R&D Systems) was used to evaluate the expression of TGF$\beta$ in the supernatant of cell cultures collected 24 hours after serum starvation. Protein analysis by immunoblotting was performed as described.[17] Human anti-E-cadherin (CDH1) (AF648; R&D Systems) and anti-vimentin (VIM) (B01P; Abnova) antibodies were used.

## GENE EXPRESSION PROFILING

Total RNA, including lncRNA and micro RNA (miRNA, miR), was purified with an miRNAeasy kit (Qiagen). Genome-wide expression profiling was performed using the low-input QuickAmp labeling kit and human SurePrint G3 8x60K probes pangenomic microarrays (Agilent Technologies, Santa Clara, CA) as described.[15] These microarrays include 26,083 Entrez genes and 30,606 lncRNAs. Gene expression data were processed using Feature Extraction and GeneSpring software (Agilent Technologies). Microarray data sets have been deposited into the public Gene Expression Omnibus database under accession numbers GSE102109 and GSE102110. Gene set enrichment analysis (GSEA) was performed using the Java tool developed at the Broad Institute (Cambridge, MA). The *Enrichr* algorithm (http://amp.pharm.mssm.edu/Enrichr) was also used to identify key genes associated with relevant signaling pathways.

## QUANTITATIVE REVERSE-TRANSCRIPTION POLYMERASE CHAIN REACTION

Quantitative reverse-transcription polymerase chain reaction (Q-RT-PCR) was performed as described[16] by using a SYBR Green master mix (Applied Biosystems, Carlsbad, CA). A mixture of deoxythymidine oligomer (250 ng) and random hexamers (100 ng) was used to prime the RT reaction of 1 µg total RNA (Superscript III RT; Invitrogen). A list of DNA primers used in this study is provided in Supporting Table S2.

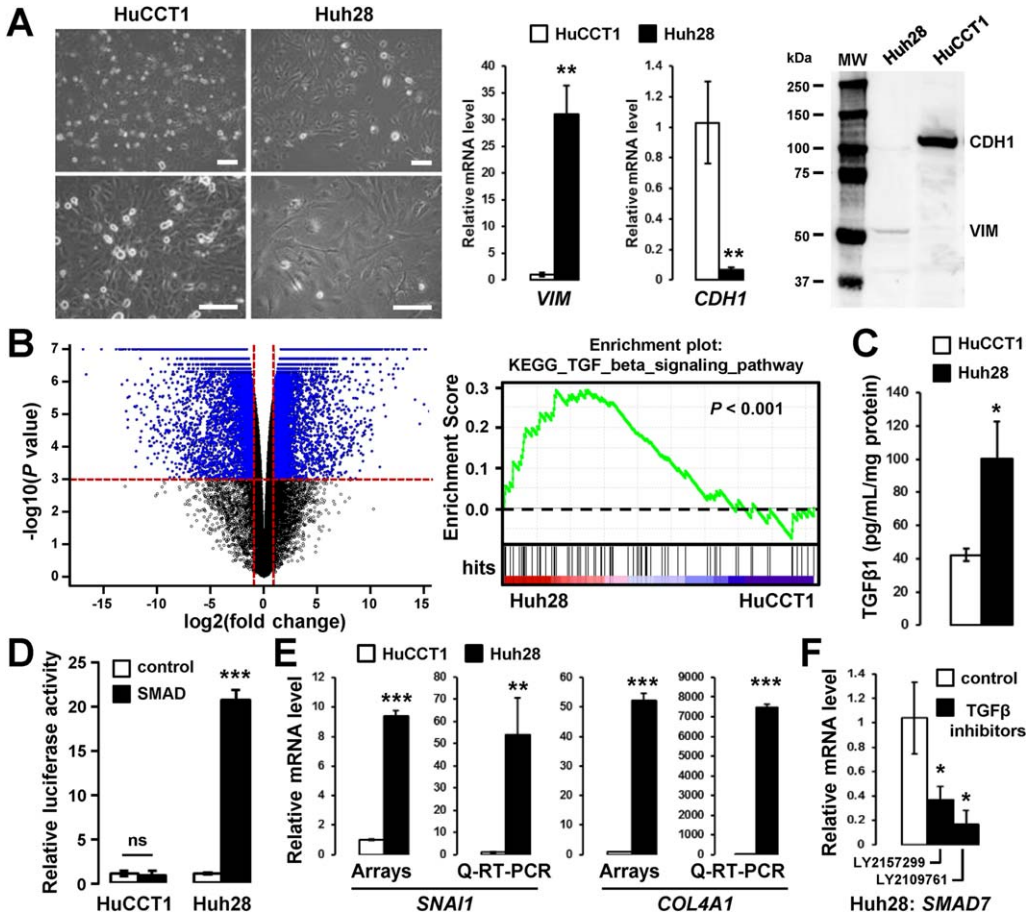


**FIG. 1.** HuCCT1 and Huh28 cell lines exhibit an epithelioid and a mesenchymal-like phenotype respectively, the later correlating with endogenous activation of the TGF$\beta$ pathway. (A) Phase contrast micrographs of HuCCT1 and Huh28 cells (left panel; scale bar, 100 µm) and expression of vimentin and E-cadherin at the RNA (middle panel) and protein level (right panel). (B) Volcano plot of genes differentially expressed between HuCCT1 and Huh28 (left panel) and GSEA highlighting a TGF$\beta$ signature enriched in the gene expression profile of Huh28. (C) Enzyme-linked immunosorbent assay demonstrating increased secretion of TGF$\beta$1 in the supernatant of Huh28 cells 24 hours after overnight serum starvation. (D) Relative luciferase activity of HuCCT1 and Huh28 engineered cell lines in which a luciferase gene is under the transcriptional control of a TATA box alone (white bars) or with SMAD responsive elements (black bars). Luciferase activity was measured at the basal level without exogenous addition of TGF$\beta$ after overnight serum starvation. (E) Gene expression analysis of TGF$\beta$ target genes in HuCCT1 and Huh28 cells at the basal level by microarray and Q-RT-PCR. (F) Q-RT-PCR analysis of TGF$\beta$ target gene *SMAD7* in Huh28 cells treated with 10 µM TGF$\beta$ inhibitors (black bars). Statistical analysis was performed by *t* test ($^{*}P < 0.05$; $^{**}P < 0.01$; $^{***}P < 0.001$); n $\geq$ 3 replicates. Data represent mean ± SD. Abbreviations: mRNA, messenger RNA; MW, molecular weight.

## FUNCTIONAL TESTS

Cell viability was evaluated using a PrestoBlue reagent (Invitrogen). Data were expressed as relative cell viability compared to untreated cells transfected with the control plasmid set as 1. Cell migration and invasion were evaluated using BD BioCoat Matrigel Invasion Chambers (BD Biosciences) as described.[16] Briefly, $4 \times 10^4$ cells were plated in serum-free medium either on an 8-µm pore-size positron emission tomography membrane insert coated with a layer of matrigel basement membrane matrix (invasion test) or on an 8-µm pore-size positron emission tomography control membrane insert (migration test). The lower compartment contained medium with 10% fetal bovine serum as a chemoattractant. After incubation for 48 hours, we removed the cells remaining on the upper surface of the membrane with a cotton swab, fixed cells in 4% paraformaldehyde that had passed through to the lower surface of the membrane, and stained the fixed cells with 1% crystal violet. We scored invasive and migrating cells per membrane under a

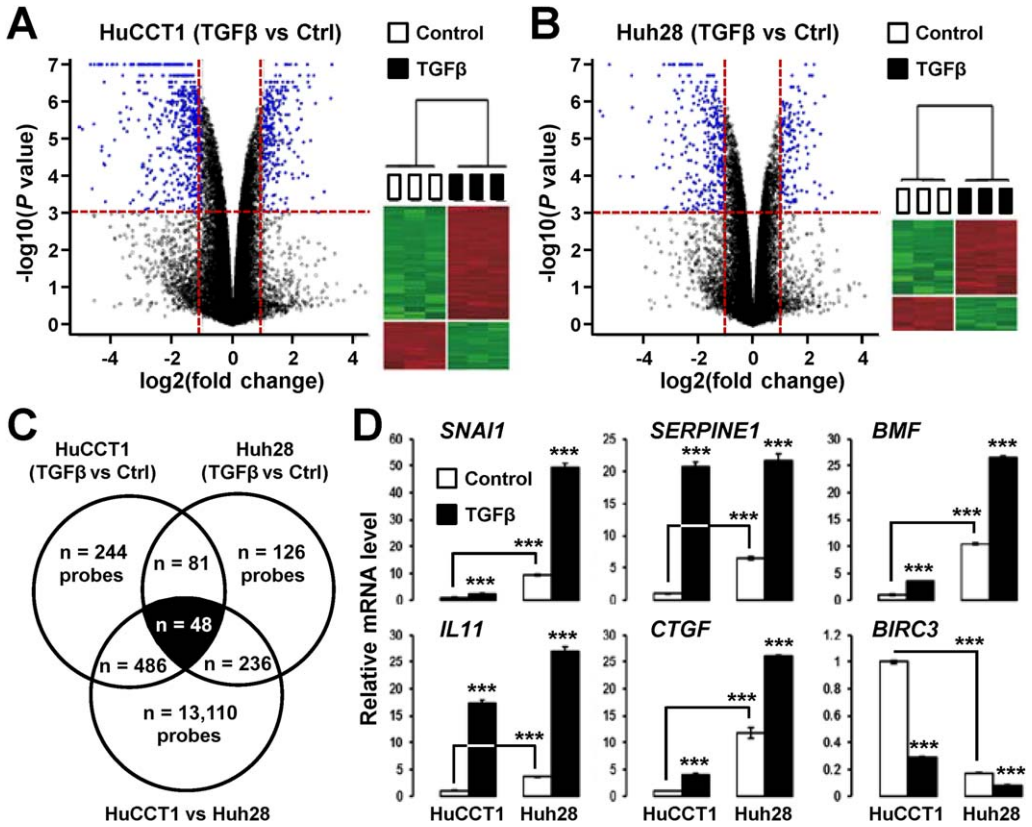


**FIG. 2.** A TGF$\beta$-specific gene expression signature in cholangiocarcinoma cell lines. (A,B) Volcano plot and hierarchical clustering of genes differentially expressed by TGF$\beta$ (1 ng/mL, 16 hours) in (A) HuCCT1 and (B) Huh28 cells. Horizontal dashed lines on volcano plots, $P < 0.001$; vertical dashed lines, fold change >2. (C) Venn diagram analysis of genes differentially expressed by TGF$\beta$ in HuCCT1 and Huh28 cells. A common TGF$\beta$ signature made of 48 probes (42 nonredundant well-annotated genes) was identified. (D) Expression of six well-known TGF$\beta$ target genes in HuCCT1 and Huh28 cells after 16 hours of culture in absence (white bars) or presence (black bars) of 1 ng/mL TGF$\beta$. Statistical analysis was performed by *t* test (*$P < 0.05$; **$P < 0.01$; ***$P < 0.001$); n ≥ 3 replicates. Data represent mean ± SD. Abbreviation: Ctrl, control.

light microscope at a 5 × magnification (n = 3 independent experiments). The number of migrating and invasive cells after transfection of TLINC was normalized relative to the number of migrating and invasive cells after transfection of the control plasmid, which was set to 1.

## HUMAN iCCA SAMPLES AND TISSUE MICROARRAY

Freshly frozen and formalin-fixed paraffin-embedded human iCCA samples were obtained through the national liver biobanks network. Written informed consent was obtained from all patients. The study protocol fulfilled national laws and regulations and was approved by the local ethics committee and the institutional review board of the Institut National de la Santé et de la Recherche Médicale (IRB00003888). Tissue microarrays were performed using a Minicore 3 Tissue Arrayer (Excilone, Vicq, France) as described.[6]

## LASER CAPTURE MICRODISSECTION

Laser capture microdissection (LCM) was performed using an Arcturus Veritas Microdissection system (Applied Biosystems) as described.[6] Briefly, serial sections of 10-μm frozen tissues were mounted onto PEN membrane glass slides prior to LCM of biliary epithelial cells and fibrous tissue from tumor and nontumor parts. Total RNA was purified using an Arcturus Picopure RNA isolation kit (Applied Biosystems).

## TABLE 1. TGFβ SIGNATURE IN CHOLANGIOCARCINOMA CELL LINES

(A) Genes induced by TGFβ

| Agilent Probe | Gene Name | Gene Symbol | Accession No. | HuCCT1 (TGFβ/Ctrl) | | Huh28 (TGFβ/Ctrl) | | Huh28/HuCCT1 | | Known TGFβ Target |
|---|---|---|---|---|---|---|---|---|---|---|
| | | | | *P* Value | FC | *P* Value | FC | *P* Value | FC | |
| A_24_P411561 | Hepatitis A virus cellular receptor 2 | HAVCR2 | NM_032782 | 1.00E-07 | 38.46 | 5.00E-07 | 7.14 | 1.40E-06 | 11.25 | yes |
| A_24_P158089 | Serpin peptidase inhibitor, clade E (nexin, plasminogen activator inhibitor type 1), member 1 | SERPINE1 | NM_000602 | < 1e-07 | 20.83 | 7.00E-07 | 3.33 | 1.00E-07 | 6.63 | yes |
| A_21_P0011334 | na | XLOC_l2_004757 | BC043257 | 4.50E-05 | 18.52 | < 1e-07 | 5.88 | 8.21E-04 | 5.20 | no |
| A_33_P3243887 | Interleukin 11 | IL11 | NM_000641 | < 1e-07 | 17.24 | < 1e-07 | 7.14 | 1.40E-06 | 3.54 | yes |
| A_21_P0001676 | na | XLOC_000166 | na | < 1e-07 | 15.15 | 5.10E-06 | 2.08 | < 1e-07 | 300.67 | no |
| A_23_P153571 | IGF-like family member 2 | IGFL2 | NM_001002915 | 3.40E-06 | 12.82 | 5.35E-05 | 2.27 | 4.69E-05 | 5.42 | no |
| A_33_P3243454 | IGF-like family member 3 | IGFL3 | NM_207393 | 5.30E-06 | 11.76 | 1.00E-07 | 3.70 | 4.00E-07 | 57.37 | no |
| A_33_P3255384 | BPI Fold Containing Family C | BPIFC | NM_174932 | 1.00E-07 | 10.20 | 7.56E-05 | 2.78 | 2.00E-07 | 12.20 | no |
| A_32_P185637 | Collagen, type XX, alpha 1 | COL20A1 | NM_020882 | 1.50E-06 | 10.10 | < 1e-07 | 6.25 | 3.10E-06 | 8.09 | no |
| A_23_P110777 | Leukocyte cell-derived chemotaxin 2 | LECT2 | NM_002302 | 2.57E-04 | 8.33 | 1.23E-05 | 7.69 | 2.30E-06 | 7.21 | no |
| A_33_P3345534 | Keratin 14 | KRT14 | NM_000526 | 1.00E-07 | 7.69 | 9.30E-06 | 2.70 | 1.00E-07 | 10.82 | no |
| A_23_P96158 | Keratin 17 | KRT17 | NM_000422 | < 1e-07 | 7.69 | 8.70E-06 | 2.63 | < 1e-07 | 9.50 | no |
| A_24_P887857 | na | na | na | < 1e-07 | 7.69 | 1.65E-05 | 2.70 | 1.00E-07 | 9.67 | no |
| A_23_P205074 | Solute carrier family 46, member 3 | SLC46A3 | NM_181785 | 3.15E-04 | 7.69 | 1.00E-06 | 2.33 | 3.55E-04 | 7.54 | no |
| A_24_P882732 | na | na | DR007925 | < 1e-07 | 7.14 | 2.28E-05 | 2.70 | 1.00E-07 | 9.50 | no |
| A_21_P0011578 | na | XLOC_l2_006021 | DB117598 | 3.00E-07 | 7.14 | 3.00E-05 | 2.70 | 4.00E-07 | 8.77 | no |
| A_33_P3857239 | Keratin 42 pseudogene | KRT42P | NR_033415 | < 1e-07 | 6.67 | 9.70E-06 | 2.86 | 1.00E-07 | 8.69 | no |
| A_33_P3235905 | na | na | na | 6.20E-05 | 6.67 | 6.82E-05 | 2.44 | 3.22E-04 | 3.90 | no |
| A_21_P0008663 | na | XLOC_011331 | na | 2.90E-06 | 6.67 | < 1e-07 | 5.56 | 3.00E-07 | 19.21 | no |
| A_32_P62963 | Keratin 16 pseudogene 2 | KRT16P2 | NR_029392 | 1.00E-07 | 5.88 | 2.19E-05 | 2.70 | 4.00E-07 | 5.88 | no |
| A_23_P381489 | Long intergenic nonprotein coding RNA 313 | LINC00313 | NR_026863 | 4.10E-06 | 5.88 | 8.91E-05 | 2.08 | 2.19E-04 | 2.29 | no |
| A_23_P166779 | Long intergenic nonprotein coding RNA 312 | LINC00312 | NR_024065 | 3.06E-05 | 4.17 | 1.00E-07 | 5.00 | 1.36E-04 | 2.86 | no |
| A_23_P19663 | Connective tissue growth factor | CTGF | NM_001901 | 4.00E-07 | 4.00 | 1.91E-05 | 2.22 | 1.00E-07 | 11.67 | yes |
| A_19_P00321671 | na | na | na | 1.56E-04 | 4.00 | 3.60E-06 | 3.03 | 5.06E-05 | 5.57 | no |
| A_21_P0012601 | na | XLOC_l2_010751 | na | 1.20E-06 | 4.00 | 6.60E-06 | 3.03 | 5.00E-07 | 5.23 | no |
| A_32_P76627 | na | na | CR597597 | 1.00E-07 | 3.70 | 2.60E-06 | 2.78 | 3.00E-07 | 4.00 | no |
| A_23_P379649 | Bcl2 modifying factor | BMF | NM_001003940 | 1.65E-05 | 3.57 | 3.00E-07 | 2.56 | 8.00E-07 | 10.75 | yes |
| A_21_P0009087 | na | XLOC_012049 | na | 1.72E-04 | 3.45 | 1.06E-05 | 3.03 | 2.81E-05 | 5.86 | no |
| A_19_P00318323 | Long intergenic nonprotein coding RNA 340 | LINC00340 | NR_015410 | 2.06E-05 | 3.33 | 8.60E-06 | 2.27 | 1.00E-07 | 19.17 | no |
| A_23_P107744 | Sphingosine-1-phosphate receptor 5 | S1PR5 | NM_030760 | 6.04E-04 | 3.03 | 1.50E-06 | 3.57 | 1.35E-05 | 12.24 | no |
| A_32_P309404 | Solute carrier family 22 (extraneuronal monoamine transporter), member 3 | SLC22A3 | NM_021977 | 5.00E-07 | 3.03 | 1.78E-05 | 2.04 | 1.60E-06 | 3.48 | no |
| A_24_P838448 | Long intergenic nonprotein coding RNA 340 | LINC00340 | NR_015410 | 1.04E-04 | 2.86 | 1.30E-06 | 2.44 | 2.00E-07 | 12.50 | no |

**TABLE 1.** *CONTINUED*

(A) Genes induced by TGF$\beta$

| Agilent Probe | Gene Name | Gene Symbol | Accession No. | HuCCT1 (TGF$\beta$/Ctrl) | | Huh28 (TGF$\beta$/Ctrl) | | Huh28/HuCCT1 | | Known TGF$\beta$ Target |
|---|---|---|---|---|---|---|---|---|---|---|
| | | | | *P* Value | FC | *P* Value | FC | *P* Value | FC | |
| A_23_P124642 | RAS guanyl releasing protein 1 (calcium and DAG-regulated) | RASGRP1 | NM_005739 | 1.40E-05 | 2.70 | 1.32E-05 | 2.08 | < 1e-07 | 27.00 | no |
| A_23_P344531 | Synaptopodin | SYNPO | NM_007286 | 7.10E-06 | 2.50 | 1.60E-06 | 2.56 | < 1e-07 | 24.38 | no |
| A_23_P303548 | Nucleolar protein 4-like | NOL4L | XM_003403733 | 2.34E-04 | 2.44 | 5.14E-05 | 2.08 | 4.81E-04 | 2.31 | no |
| A_24_P239606 | Growth arrest and DNA-damage-inducible, beta | GADD45B | NM_015675 | 3.00E-06 | 2.33 | 6.10E-05 | 2.44 | 3.69E-05 | 2.93 | yes |
| A_23_P131846 | Snail homolog 1 (*Drosophila*) | SNAI1 | NM_005985 | 4.20E-06 | 2.33 | 1.00E-07 | 5.26 | < 1e-07 | 9.48 | yes |
| A_21_P0009196 | na | XLOC_012515 | na | 6.91E-04 | 2.27 | 2.06E-05 | 2.08 | 8.00E-06 | 7.67 | no |

(B) Genes repressed by TGF$\beta$

| Agilent Probe | Gene Name | Gene Symbol | Accession No. | HuCCT1 (TGF$\beta$/Ctrl) | | Huh28 (TGF$\beta$/Ctrl) | | Huh28 / HuCCT1 | | Known TGF$\beta$ Target |
|---|---|---|---|---|---|---|---|---|---|---|
| | | | | *P* Value | FC | *P* Value | FC | *P* Value | FC | |
| A_33_P3663974 | Thyroid hormone receptor beta | THRB | NM_001128177 | 8.10E-06 | 0.49 | 1.75E-04 | 0.47 | 1.70E-06 | 0.42 | no |
| A_21_P0010449 | na | XLOC_014399 | XR_109732 | 2.70E-06 | 0.47 | 1.05E-04 | 0.38 | 1.00E-07 | 0.08 | no |
| A_21_P0000841 | Hypothetical LOC100505483 | LOC100505483 | NR_038926 | 7.60E-06 | 0.45 | 3.13E-05 | 0.40 | 2.25E-05 | 0.43 | no |
| A_23_P121064 | Pentraxin 3, long | PTX3 | NM_002852 | 1.50E-06 | 0.45 | 2.00E-06 | 0.32 | 4.90E-06 | 0.42 | yes |
| A_23_P121657 | Heparan sulfate (glucosamine) 3-O-sulfotransferase 1 | HS3ST1 | NM_005114 | 3.00E-07 | 0.42 | 3.07E-04 | 0.45 | < 1e-07 | 0.00 | no |
| A_23_P52266 | Interferon-induced protein with tetratricopeptide repeats 1 | IFIT1 | NM_001548 | 1.19E-04 | 0.40 | 1.66E-05 | 0.36 | 1.72E-05 | 0.27 | no |
| A_23_P345460 | Pleckstrin homology domain-containing, family G (with RhoGef domain) member 4 | PLEKHG4 | NM_015432 | 6.00E-07 | 0.36 | 2.90E-04 | 0.50 | 1.00E-07 | 0.21 | no |
| A_23_P98350 | Baculoviral inhibitor of apoptosis protein repeat-containing 3 | BIRC3 | NM_001165 | 1.00E-07 | 0.29 | 2.70E-06 | 0.45 | < 1e-07 | 0.17 | yes |
| A_33_P3398181 | Hypothetical LOC100127909 | LOC100127909 | XR_111781 | 8.81E-05 | 0.26 | 7.13E-05 | 0.35 | 1.89E-05 | 0.27 | no |
| A_23_P415021 | Methyltransferase-like 7A | METTL7A | NM_014033 | 2.00E-07 | 0.22 | 4.00E-06 | 0.32 | 1.00E-07 | 0.19 | no |

Abbreviations: Ctrl, control; FC, fold change; na, not applicable.

## *IN SITU* HYBRIDIZATION

Specific *in situ* hybridization (ISH) riboprobes were designed to evaluate the expression of TLINC-S and TLINC-T transcripts (Supporting Table S1). Sense and antisense riboprobes were generated by *in vitro* transcription from PCR products incorporating the promoter of T7 RNA polymerase. *In vitro* transcription was performed with 40 units T7 RNA Polymerase (Agilent) in the presence of 0.35 mM digoxygenin-11-UTP (Roche Diagnostics, Meylan, France). ISH was performed on the Discovery Automated IHC Stainer using the Ventana Detection Kit (Ventana Medical Systems, Tucson, AZ). Staining was performed using an anti-digoxygenin-horseradish peroxidase antibody (Roche Diagnostics), and signal detection was performed using a nitro-blue tetrazolium/5-bromo-4-chloro-3′-indolyphosphate or a Discovery purple kit (Ventana Medical Systems).

## CIRCULAR RNA ANALYSIS

RT-PCR using convergent and divergent primers combined with ribonuclease (RNase) R (Epicentre, Middleton, WI) treatment (1 μ/μg, 37 °C, 1 hour) was used to detect linear and circular transcripts of *TLINC* and actin beta (*ACTB*). The sequence of DNA primers is provided in Supporting Table S2.

# Results

## ENDOGENOUS TGF*β* ACTIVATION IN Huh28 CELLS

HuCCT1 and Huh28 cells were used to study the impact of TGF*β* on iCCA cells. The two cell lines have different phenotypic features that reflect tumor heterogeneity. HuCCT1 cells exhibit an epithelioid-like phenotype associated with a cobblestone-like morphology and numerous cell-to-cell junctions compared to Huh28 cells, which exhibit a mesenchymal-like phenotype associated with a spindle and polygonal morphology together with prominent cytoskeleton fibers (Fig. 1A). Epithelioid and mesenchymal-like phenotypes were further characterized by the expression of *CDH1* and *VIM* markers in HuCCT1 cells and Huh28 cells, respectively, both at the RNA and protein level (Fig. 1A). Marked differences in pangenomic expression profiles were also highlighted between HuCCT1 and Huh28 cells and validated by Q-RT-PCR (Fig. 1B; Supporting Fig. S1A). Interestingly, GSEA, using the Kyoto Encyclopedia of Genes and Genomes signaling pathways, demonstrated that a TGF*β* signature was significantly enriched ($P < 0.001$) at the basal level in mesenchymal Huh28 cells (Fig. 1B). Endogenous activation of the TGF*β* pathway in Huh28 cells was further validated by a significantly enhanced secretion of TGF*β* (Fig. 1C) that correlated with enhanced luciferase activity as detected in engineered SMAD sensor cell lines (Fig. 1D). A higher expression of TGF*β* target genes (e.g., snail family transcriptional repressor 1 [*SNAI1*], collagen type IV alpha 1 chain [*COL4A1*], *SMAD7*) in Huh28 cells was also validated by Q-RT-PCR (Fig. 1E; Supporting Fig. S1A) as well as a reduced expression of *SMAD7*, a well-known TGF*β* transcriptional target, when cells were cultured in the presence of TGF*β* inhibitors (Fig. 1F). Altogether, these data demonstrate that Huh28 cells exhibit a mesenchymal phenotype associated with basal and endogenous activation of the TGF*β* pathway.

## NEW TGF*β* TARGET GENES IN iCCA CELLS

HuCCT1 and Huh28 cells were treated with 1 ng/mL TGF*β* for 16 hours. Gene expression profiling using pangenomic microarrays identified 859 probes in HuCCT1 cells (Fig. 2A) and 491 probes in Huh28 cells (Fig. 2B) that were significantly deregulated by TGF*β* ($P < 0.001$; fold change >2). A Venn diagram analysis, including genes differentially expressed between HuCCT1 and Huh28 cells at a basal level (Fig. 1B), identified a set of 48 probes (42 nonredundant annotated genes) that were recurrently deregulated by TGF*β* in all three experimental settings (Fig. 2C; Table 1). The deregulation of well-known positive (e.g., serpin family E member 1 [*SERPINE1*], connective tissue growth factor [*CTGF*]) and negative (e.g., baculoviral inhibitor of apoptosis protein repeat containing 3 [*BIRC3*]) TGF*β* target genes was confirmed by Q-RT-PCR on independent RNA samples (Fig. 2D; Supporting Fig. S1B). GSEA was also performed in all specific gene subsets and demonstrated that the 42 common genes were significantly associated with TGF*β* and SMAD2/3 and related to EMT (Supporting Fig. S2). Importantly, this common signature comprised genes not known to be regulated by TGF*β*, including several lncRNAs (e.g., *LINC00312, LINC00340*). Notably, two microarray probes for *LINC00340* were induced by TGF*β* (Table 1).

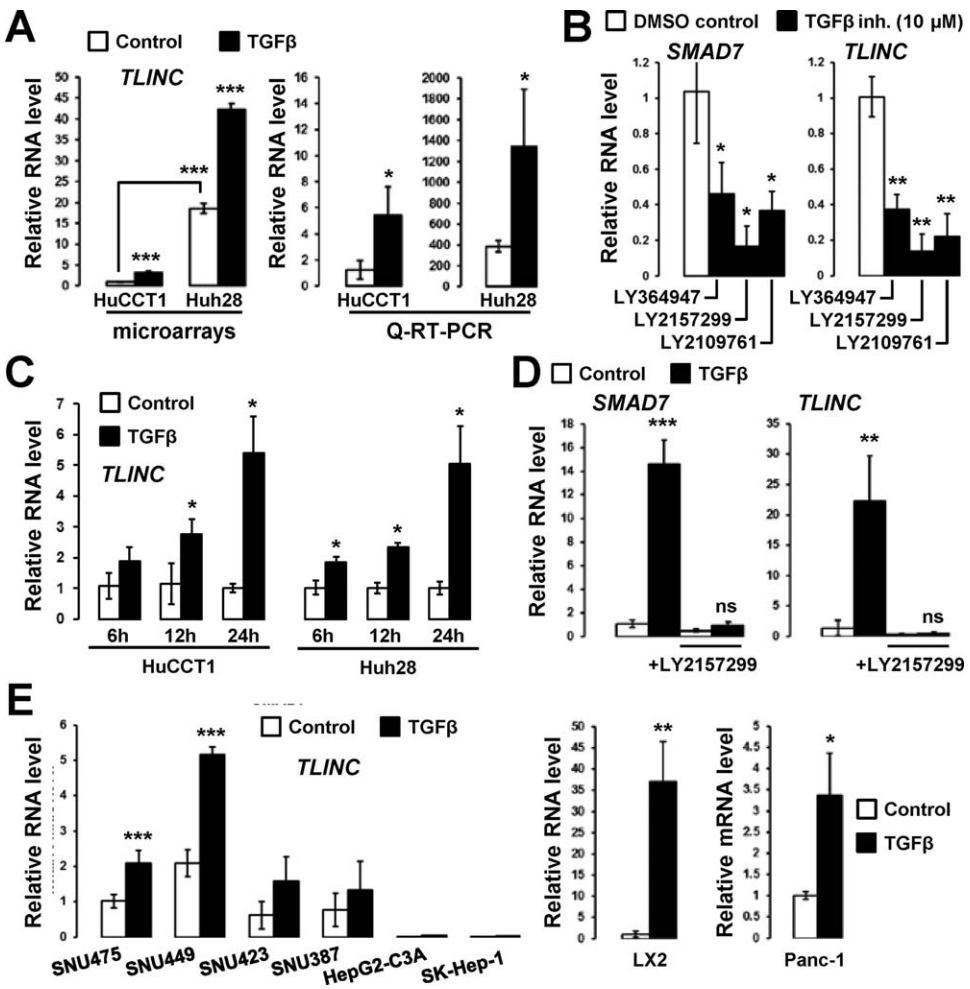


**FIG. 3.** LINC00340/CASC15/TLINC is a novel TGF$\beta$-induced lncRNA. (A) Analysis of *LINC00340* expression in HuCCT1 and Huh28 cells after 16 hours of culture in absence (white bars) or presence (black bars) of 1 ng/mL TGF$\beta$, as evaluated by microarray and Q-RT-PCR. (B) Analysis of *SMAD7* and *LINC00340* expression in Huh28 cells after 72 hours treatment with 10 μM TGF$\beta$ inhibitors. (C) Time-course analysis of *LINC00340* expression in HuCCT1 and Huh28 cells (1 ng/mL TGF$\beta$). (D) Analysis of *SMAD7* and *LINC00340* expression in primary human hepatocytes (n = 3 independent donors) in the presence of 1 ng/mL TGF$\beta$ and 10 μM TGF$\beta$ inhibitor LY2157299 for 16 hours. (E) Analysis of *LINC00340* expression in HCC cell lines (left panel) and LX2 and Panc-1 (pancreatic cancer) cells (right two panels) (1 ng/mL TGF$\beta$ for 16 hours). Statistical analysis was performed by *t* test (*$P < 0.05$; **$P < 0.01$; ***$P < 0.001$); n ≥ 3 replicates. Data represent mean ± SD. Abbreviations: DMSO, dimethyl sulfoxide; inh., inhibitor; mRNA, messenger RNA; ns, not significant.

## LINC00340/CASC15/TLINC IS A NOVEL TGF$\beta$-INDUCED lncRNA

*LINC00340* is known as cancer susceptibility candidate 15 (*CASC15*) located on chromosome 6p22. *CASC15* was reported to act as a tumor suppressor in neuroblastoma[18] and to promote tumor progression and phenotype switching in melanoma.[19] To further characterize *LINC00340* biological activities in iCCA, we first validated the microarray expression data by Q-RT-PCR. *LINC00340* was induced by TGF$\beta$ in both HuCCT1 and Huh28 cells, and a significant higher expression in Huh28 cells at the basal level was confirmed (Fig. 3A). Repression of *LINC00340* and *SMAD7* was observed in Huh28 cells treated with inhibitors of the TGF$\beta$ pathway (Fig. 3B). Time-course experiments also demonstrated increased expression of *LINC00340* by TGF$\beta$, both in HuCCT1 and Huh28 cells (Fig. 3C). Interestingly, *LINC00340* was induced by TGF$\beta$ in nontransformed human primary hepatocytes, and the induction was abolished in the presence of a TGF$\beta$ inhibitor

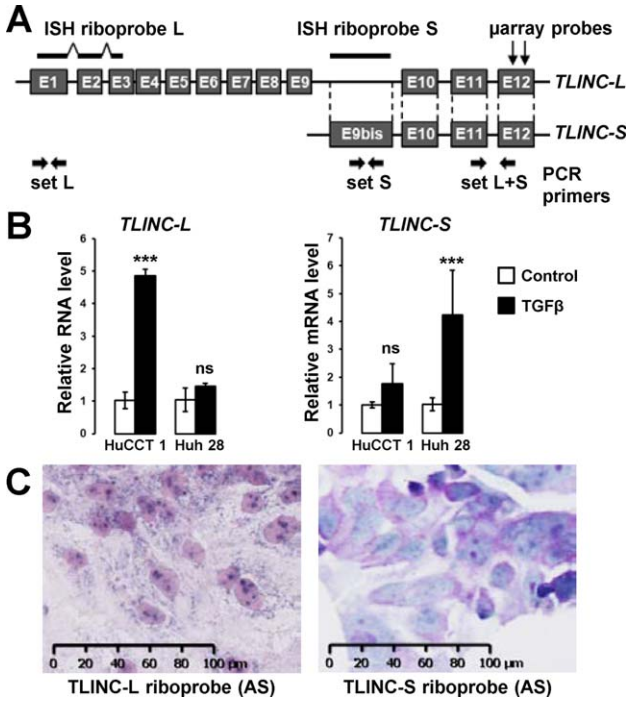


**FIG. 4.** Expression and cellular localization of TLINC isoforms. (A) Simplified representation of TLINC locus highlighting two reported isoforms: TLINC-L and TLINC-S. ISH riboprobes, sets of PCR primers, and microarray probes are also represented. (B) Analysis of *TLINC-L* and *TLINC-S* expression in HuCCT1 and Huh28 cells after 16 hours of culture in the absence (white bars) or presence (black bars) of 1 ng/mL TGF$\beta$, as evaluated by Q-RT-PCR using specific sets of primers. (C) *In situ* hybridization using TLINC-L and TLINC-S riboprobes highlights a nuclear and cytoplasmic location of both TLINC isoforms (HuCCT1 cells treated with 1 ng/mL TGF$\beta$). Scale, 100 µm. Statistical analysis was performed by *t* test ($^{*}P < 0.05$; $^{**}P < 0.01$; $^{***}P < 0.001$); n $\geq$ 3 replicates. Data represent mean ± SD. Abbreviations: (AS), antisense; mRNA, messenger RNA; ns, not significant.

(Fig. 3D). In addition, *LINC00340* was induced by TGF$\beta$ in several human HCC cell lines as well as in LX2-activated hepatic stellate cells (Fig. 3E). Finally, induction by TGF$\beta$ occurred also in nonhepatic cell lines, such as pancreatic Panc-1 (Fig. 3E). Altogether, these data demonstrate that *LINC00340* is a novel and general transcriptional target of TGF$\beta$. We therefore named it TGF$\beta$-induced lncRNA or *TLINC*.

## INDUCTION OF TWO TLINC ISOFORMS LINKED TO AN EMT PHENOTYPE

Previous studies demonstrated that *TLINC* is located on a complex locus that produces multiple transcripts by alternative splicing, including a short (TLINC-S) and a long (TLINC-L) isoform, as shown in Fig. 4A.[18,19] These two isoforms have been functionally associated with either tumor suppressive (TLINC-S)[18] or tumor promoting (TLINC-L)[19] functions in neuroblastoma and melanoma, respectively. Because our previous gene expression analysis by microarray (Fig. 2) and Q-RT-PCR (Fig. 3) could not distinguish the two isoforms (primer set L + S), we next evaluated TLINC-S and TLINC-L with specific sets of primers (Fig. 4A). TLINC-L was induced by TGF$\beta$ in HuCCT1 cells and TLINC-S in Huh28 cells, as demonstrated by Q-RT-PCR (Fig. 4B). ISH demonstrated that the two isoforms were expressed in both the cytoplasm and the nucleus (Fig. 4C).

## FUNCTIONAL CHARACTERIZATION OF TLINC ISOFORMS

Gain of function experiments were performed using DNA constructs designed to specifically overexpress TLINC-L and TLINC-S (Supporting Fig. S3A-C). No significant effect was observed on cell viability (Supporting Fig. S3D) and cell invasion (Fig. 5A); however, overexpression of TLINC-L increased cell migration (Fig. 5A). In order to get insights into the molecular mechanisms involved, gene expression profiling was performed on HuCCT1 cells after TLINC-L overexpression. Numerous genes were repressed (Fig. 5B), whereas several inflammation-associated genes, including cytokines and chemokines (e.g., *IL6, IL8*, C-X-C motif chemokine ligand 1 [*CXCL1*]) were induced together with *LINC00340/TLINC* (Fig. 5B). Accordingly, an immune response gene signature was significantly enriched in the gene expression profiles of HuCCT1 cells overexpressing TLINC-L (Fig. 5C; Supporting Table S3). The enrichment of a described[20] cell migration signature supported the phenotype observed after TLINC-L overexpression (Fig. 5C). Although no obvious change was observed on cell morphology after TLINC-L transfection, EMT-associated *SNAI2* was enriched in the gene expression profiles of TLINC-L transfected cells (Supporting Table S4). A significant enrichment of TGF$\beta$ target genes was also observed, suggesting that TLINC-L may act as a feedback regulator of the TGF$\beta$ pathway (Fig. 5C). However, experimental data using SMAD sensor cell lines refuted this hypothesis (Supporting Fig. S3E). In agreement

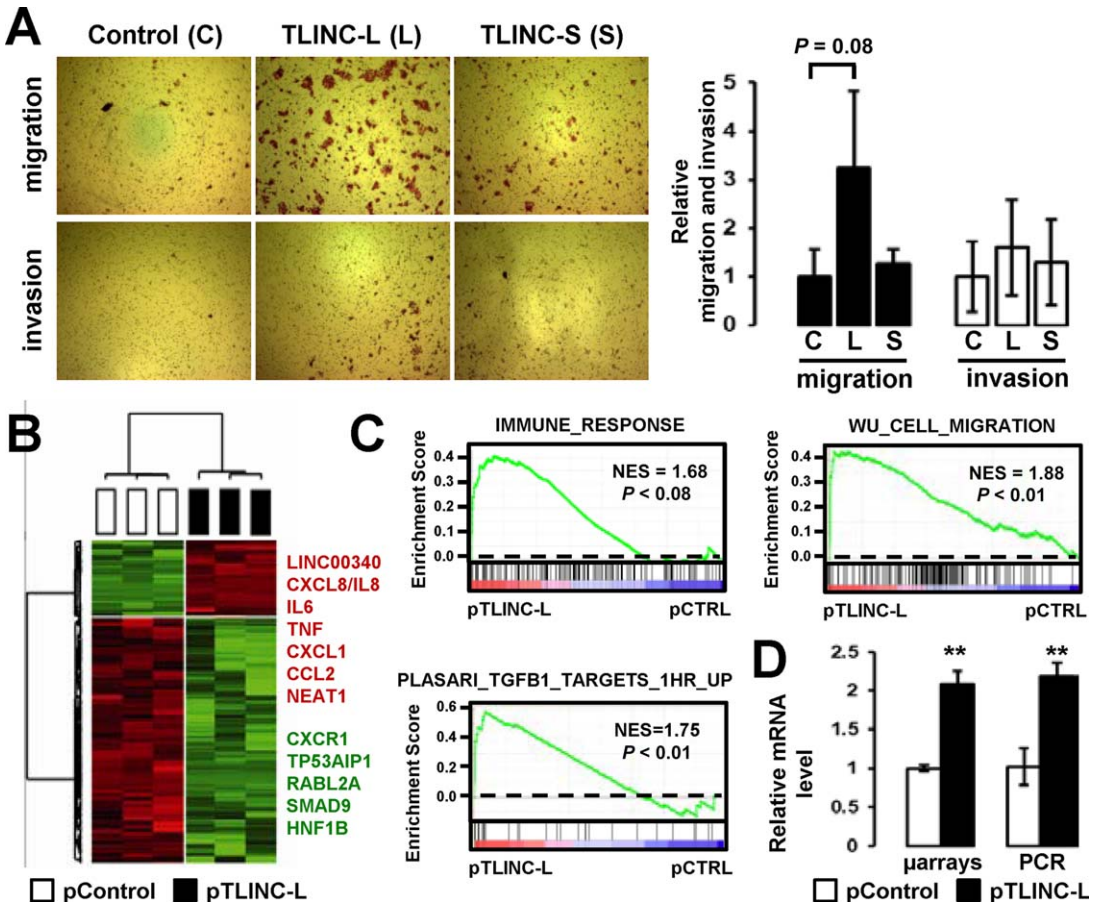


**FIG. 5.** Functional analysis of TLINC. (A) Effects of TLINC-L and TLINC-S overexpression on migration and invasion of HuCCT1 cells 48 hours after transfection of the DNA constructs. (B) Gene expression analysis of HuCCT1 cells 24 hours after transfection of the *TLINC-L* DNA construct. Hierarchical clustering was based on the expression of 431 genes ($P < 0.01$; fold change >1.5). (C) GSEA of specific signatures significantly enriched in the gene expression profile of HuCCT1 cells overexpressing TLINC-L. (D) Analysis of *IL8* expression in HuCCT1 cells after transfection of the *TLINC-L* DNA construct, as evaluated by microarray and Q-RT-PCR. Statistical analysis was performed by *t* test ($^{*}P < 0.05$; $^{**}P < 0.01$; $^{***}P < 0.001$); $n \geq 3$ replicates. Data represent mean ± SD. Abbreviations: C, control; CCL2, chemokine (C-C motif) ligand 2; CTRL, control; CXCR1, chemokine (C-X-C motif) receptor 1; HNF, hepatocyte nuclear factor; L, long; mRNA, messenger RNA; NES, normalized enrichment score; p, plasmid [for pControl and pTLINC-L]; RABL2A, RAB, member of RAS oncogene family like 2A; S, short; TP53AIP1, tumor protein p53 regulated apoptosis inducing protein 1; TNF, tumor necrosis factor.

with the identified immune signature, increased expression of *IL8* was confirmed after TLINC overexpression (Fig. 5D). As a potent inducer of cell motility, *IL8* may contribute to the observed phenotype by creating a gradient for the migration of cancer cells.

## INCREASED EXPRESSION OF TLINC IN HUMAN iCCA

We next evaluated the clinical relevance of TLINC expression in human resected iCCA. TLINC was shown to be induced both in tumor biliary epithelial cells and in the stroma compared to their nontumor counterparts (Fig. 6A). Overexpression of TLINC in iCCA tumors was validated by ISH on tissue microarrays (Fig. 6A). Interestingly, Q-RT-PCR on 22 resected human iCCA demonstrated that the expression of TLINC-L and TLINC-S was tightly correlated (Fig. 6B). A detailed analysis by ISH on human resected iCCA confirmed that both TLINC isoforms were expressed in tumor cholangiocytes and in cells from the tumor microenvironment. In the nontumor liver, TLINC was only expressed in remodeled portal areas with signs of ductular reaction and inflammation (Fig. 6C; Supporting Fig. S4).

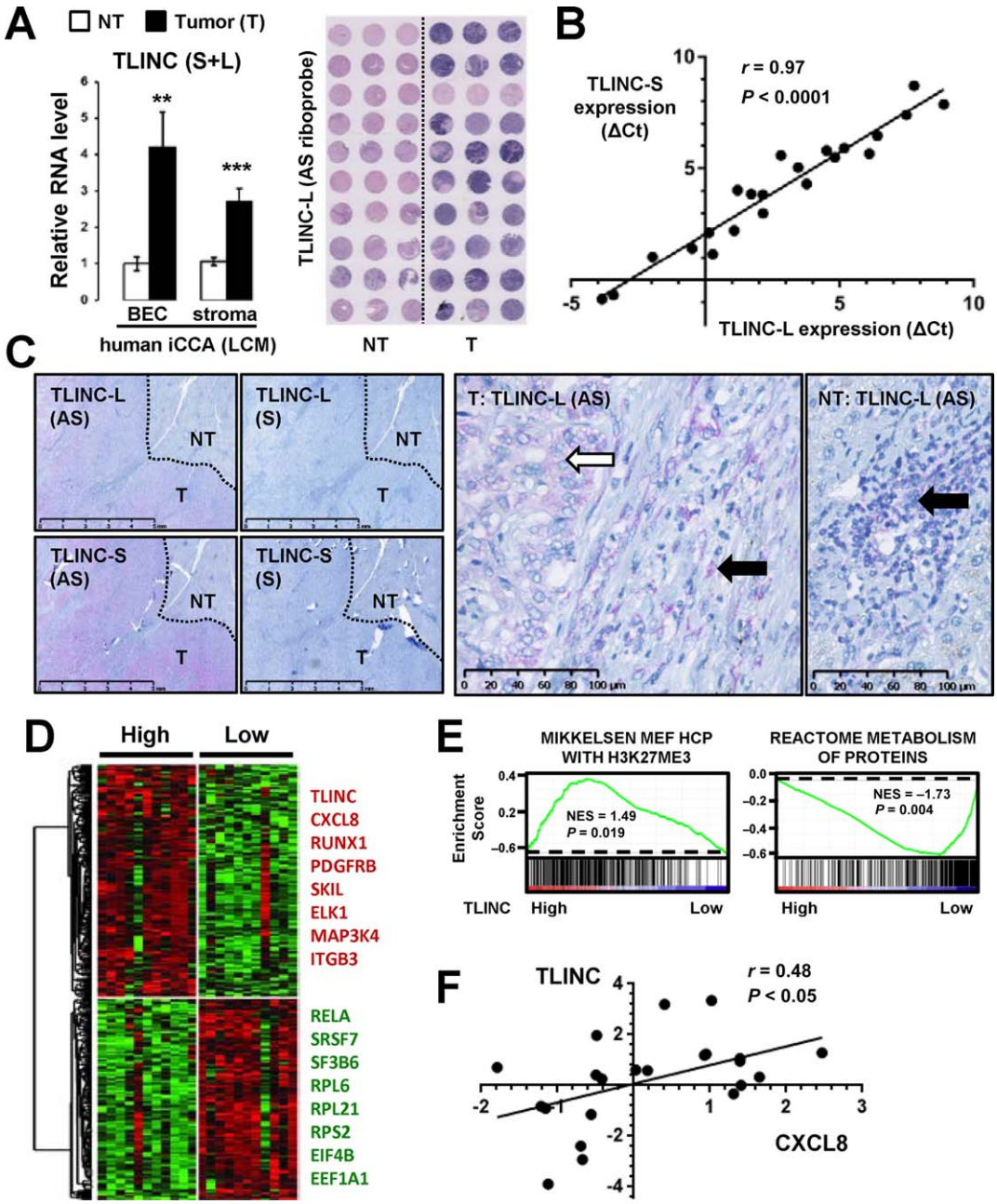


**FIG. 6.** Clinical relevance of TLINC expression in human resected iCCA. (A) Analysis of *TLINC* expression in biliary epithelial cells and stroma isolated by laser capture microdissection from nontumor (white bars) and tumor (black bars) tissues (n = 10 patients, left panel). Data represent mean ± SD. ISH on human iCCA tissue microarrays using TLINC-L antisense riboprobes demonstrating higher expression in the tumor than in the nontumoral tissues (tissue microarray, right panel). (B) Correlation between *TLINC-L* and *TLINC-S* expression in human iCCA resected tumors, as evaluated by Q-RT-PCR (n = 22 patients). (C) ISH analysis of *TLINC-L* and *TLINC-S* expression using specific antisense and sense riboprobes. In the tumor part, TLINC was expressed in both epithelial cells (white arrow) and in the stroma (black arrow). In the nontumor part, TLINC was only expressed in remodeled portal areas with signs of ductular reaction. Scale bars: 5 mm (left panels) and 100 μm (right panels). (D) Expression of TLINC identifies human iCCA with specific gene expression profiles. Median expression of TLINC was used to define high and low expression groups (n = 22 patients). (E) Example of signatures significantly enriched in the gene expression profiles of iCCA with high versus low TLINC expression, as evaluated by GSEA. (F) Correlation between the expression of TLINC and CXCL8 in 22 human iCCAs. Abbreviations: (AS), antisense; BEC, biliary epithelial cells; EEF1A1, eukaryotic translation elongation factor 1 alpha 1; EIF4B, eukaryotic translation initiation factor 4B; ELK1, ELK1, ETS transcription factor; ITGB3, integrin subunit beta 3; HCP, high-CpG-density promoters; MAP3K4, mitogen-activated protein kinase kinase kinase 4; MEF, mouse embryonic fibroblast; NF-kB subunit; NES, normalized enrichment score; NT, nontumor; PDGFRB, platelet derived growth factor receptor beta; RELA, RELA proto-oncogene; RPL6, ribosomal protein L6; RPL21, ribosomal protein L21; RPS2, ribosomal protein S2; RUNX1, runt related transcription factor 1; (S), sense; SF3B6, splicing factor 3b subunit 6; SKIL, SKI like proto-oncogene; SRSF7, serine and arginine rich splicing factor 7; T, tumor.

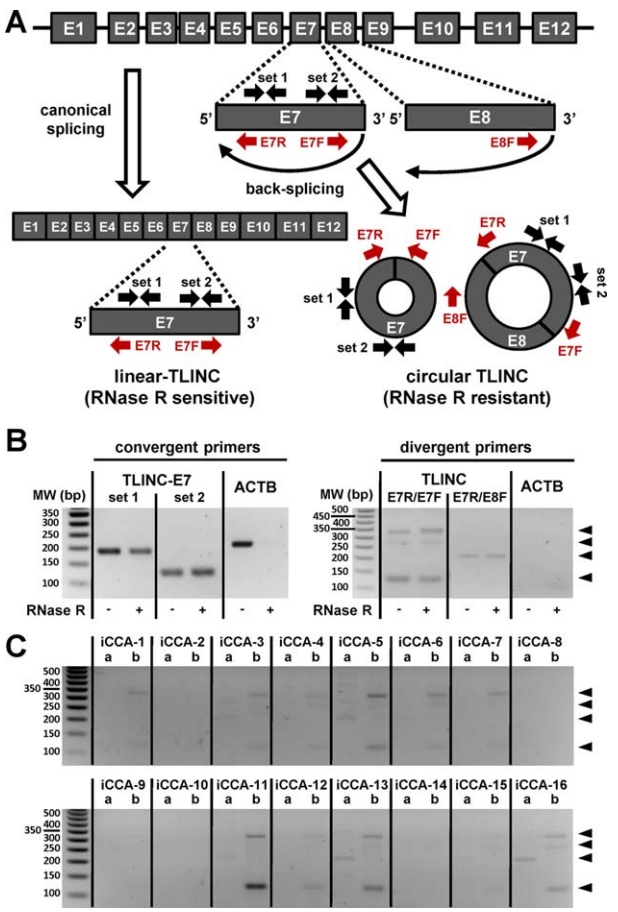


**FIG. 7.** Experimental evidence of TLINC circular isoforms. (A) Schematic representation of TLINC RNA processing into linear RNA (canonical splicing) or circular RNA (back-splicing). Several sets of convergent and divergent PCR primers were designed to detect specific linear and circular isoforms. (B) RNA was extracted from Huh28 cells after 16 hours of treatment with 1 ng/mL TGF$\beta$. RNase R treatment was performed prior to RT-PCR analysis. Convergent primers (left panel) detected specific TLINC-E7 transcripts in both RNase R untreated and treated samples. For *ACTB* (a housekeeping gene highly expressed), no amplification was observed after RNase R treatment. By using a specific set of divergent primers located on exons E7 and E8, several TLINC circular isoforms were highlighted (black arrowheads). (C) RNAs were extracted from 16 human iCCA tumors. RT-PCR analysis was performed using a specific set of divergent primers located on exons E7 and E8, as indicated at the top of the panels (a, E7R/E8F; b, E7R/E7F). Black arrowheads highlight TLINC circular isoforms. Abbreviations: bp, base pair; MW, molecular weight.

## TLINC EXPRESSION DEFINES SPECIFIC SUBSETS OF HUMAN iCCA

Gene expression profiling was performed on 22 resected human iCCA, and a specific signature was defined on the basis of *TLINC* expression (Fig. 6D). High expression of *TLINC* correlated with a high expression of TGF$\beta$ target genes and inflammation-associated genes, as previously observed in cell lines (Fig. 6D; Supporting Fig. S5). In addition, GSEA demonstrated that up-regulated genes in high-TLINC-expressing tumors were significantly associated with the H3K27Me3 repressive epigenetic mark signature, while down-regulated genes were linked to protein metabolism and included numerous genes encoding ribosomal components (Fig. 6D,E; Supporting Fig. S6). Among the chemokines induced in HuCCT1 cells directly overexpressing TLINC (Fig. 5B) and possibly contributing to a migration phenotype, *IL8* was found to be significantly correlated with *TLINC* expression in human iCCA tumors (Fig. 6F).

## EXPERIMENTAL EVIDENCE OF TLINC CIRCULAR ISOFORMS

A genome-wide bioinformatic analysis of RNA-sequencing data previously reported a 204-nucleotide circular isoform of LINC00340/TLINC, probably derived from exon E7. This isoform was one of the most highly expressed circular RNAs (circRNAs) in H1-human embryonic stem cells.[21] To evaluate the putative expression of such circular isoforms in iCCA, we designed specific sets of convergent and divergent primers from exons E7 and E8 of TLINC (Fig. 7A). *ACTB* was used as a housekeeping gene control that was highly expressed and without prior evidence of a circular isoform. Interestingly, by combining RNase R treatment and RT-PCR experiments, we provide evidence of the existence of several RNase R-resistant circular TLINC isoforms not only in iCCA cells treated with TGF$\beta$ (Fig. 7B) but also in resected human iCCA tumors (Fig. 7C).

# Discussion

The molecular mechanisms involved in iCCA carcinogenesis are complex and involve multiple interactions between tumor cells and their microenvironment.[1] We previously demonstrated that active TGF$\beta$ signaling is an important feature in the iCCA microenvironment[6]; however, a deep characterization of the impact of TGF$\beta$ on tumor cells at the transcriptome level was lacking in iCCA. In this study, we first validated suitable experimental cellular models to study TGF$\beta$ signaling in iCCA cells. Particularly, we provided strong experimental evidence that Huh28 cells

exhibit an endogenous activation of TGF$\beta$, which correlates with a mesenchymal phenotype. This cell line may thus be relevant to test TGF$\beta$ inhibitors for therapeutic purposes, as was suggested in liver cancers.[22] In addition, we provided the first TGF$\beta$ transcriptomic signature in iCCA cells, which allowed us to identify novel TGF$\beta$ transcriptional targets, including coding and noncoding genes, both *in vitro* and in resected human iCCA.

Few studies have reported a deregulation of lncRNA in iCCA.[23,24] As an example, oncogenic metastasis-associated lung adenocarcinoma transcript 1 (MALAT1) lncRNA was shown to promote proliferation and invasion of CCA cell lines by activating the phosphoinositide 3-kinase/protein kinase B signaling pathway.[24] Here, we provide the first report of lncRNA directly regulated by TGF$\beta$ in iCCA, supporting the previous description of TGF$\beta$-regulated lncRNA in other cancer types.[11,12] Notably, lncRNA activated by TGF-$\beta$ was shown to induce EMT and to promote HCC cell invasion through a TGF$\beta$/miR-200/zinc finger E-box binding axis.[12] Similarly, TGF$\beta$-induced lncRNA-HIT was shown to promote EMT in breast cancer, notably by decreasing the expression of CDH1.[11] By comparing the transcriptome profiles of HuCCT1 and Huh28 cells at the basal level and after TGF$\beta$ treatment, we identified a robust signature made of 42 nonredundant genes. This signature was validated by including well-known TGF$\beta$ target genes (e.g., *SERPINE1, IL11, CTGF*, BCL2 modifying factor [*BMF*], *SNAI1*) reported in multiple cell types, including hepatocytes.[25] Importantly, this approach highlighted several novel TGF$\beta$-induced lncRNA, including LINC00312, LINC00313, and LINC00340 (TLINC), possibly involved in TGF$\beta$ signaling. LINC00312 has been reported to inhibit the migration and invasion of bladder cancer cells by targeting miR-197-3p.[26] High expression of *LINC00313* has been associated with a poor prognosis and metastasis in lung cancer.[27] Experimental data on TLINC were more complex given that several isoforms were reported to exhibit either tumor-suppressive or tumor-promoting features in various types of cancer.[18,19] Thus, in neuroblastoma, a short isoform was associated with tumor suppression by hampering cell growth and migration, and a lower expression of this short isoform was found in advanced tumors associated with a poor survival.[18] Conversely, a long isoform of TLINC was reported in metastatic melanoma and associated with tumor progression.[19] The differences in the basal expression and induction by TGF$\beta$ of TLINC isoforms in HuCCT1 and Huh28 cell lines suggest that the function of TLINC is highly dependent on the cellular context, as known for several TGF$\beta$ target genes.[10]

Although TLINC deregulation has been reported in cancer,[18,19] we provide the first evidence that TLINC is a common transcriptional target of TGF$\beta$ not only in liver cancer (iCCA and HCC) but also in other cancer types, including pancreatic cancer. Interestingly, we demonstrated that TLINC is also up-regulated by TGF$\beta$ in cells from the tumor microenvironment, as evidenced by the analysis of its expression in activated hepatic stellate cells (LX2) and in human iCCA tumors by ISH and LCM of the stroma. These data suggest that TLINC may play a role in TGF$\beta$-induced remodeling of the tumor microenvironment. Supporting this hypothesis, our experimental data show that ectopic expression of TLINC directly impacts the expression of several inflammatory mediators, including chemokine *IL8*. Increased expression of *IL8* has been reported in cancer and is associated with important changes within the tumor microenvironment, including promotion of angiogenesis, infiltration of neutrophils and tumor-associated macrophages, and migration of cancer cells.[28,29] Interestingly, a functional link has been established between the expression of *IL8* and nuclear paraspeckle assembly transcript 1 [*NEAT1*], another lncRNA that we found to be induced in cells transfected with the TLINC DNA construct (Fig. 5B). Indeed, it was demonstrated that NEAT1-dependent relocation of a splicing factor proline/glutamine-rich from the promoter region of the *IL8* gene to paraspeckle led to the transcriptional activation of *IL8*.[30] One can hypothesize that TLINC acts as a structural component of paraspeckles and that interaction with NEAT1 may result in *IL8* expression. This hypothesis is in agreement with the partial nuclear location of TLINC. The enrichment of a gene signature associated with repressive marks H3K27me3 in iCCA tumors characterized by a high expression of TLINC may also suggest a role of TLINC in epigenetic silencing, as was described for other lncRNAs, such as Kcnq1ot1 antisense.[31] Similarly, enrichment of a gene signature associated with protein metabolism in iCCA with low TLINC expression together with the cytoplasmic expression of TLINC may suggest a role of TLINC in translation, as described for lncRNA growth arrest specific 5 (GAS5), which interacts with the translational machinery to inhibit c-Myc translation.[32] Another interesting aspect is the restricted expression of TLINC in remodeled portal areas with

signs of ductular reaction in nontumor livers. These areas are usually associated with activation of the cancer stem cell compartment.[33] Supporting a putative role of TLINC in cancer stem cell biology, TLINC has been reported to be highly expressed in human embryonic stem cells.[21,34] At the functional level, we showed that TLINC-L overexpression in HuCCT1 cells resulted in increased cell migration. Although the underlying molecular mechanisms are still to be clarified, *SNAI2* was found to be enriched in the gene expression profiles of TLINC-L transfected cells, suggesting that the type of migration could be partly related to EMT. Other genes found to be tightly correlated with TLINC expression in human iCCA tumors may also contribute to the observed phenotypes. As an example, platelet-derived growth factor receptor beta (*PDGFRB*) has been associated with the aggressive behavior of several types of tumors.[35] Notably, PDGFRB has been shown to promote liver metastasis formation of mesenchymal-like colorectal tumor cells.[36]

Finally, we provide experimental evidence of circular isoforms of TLINC that may represent putative, relevant, noninvasive biomarkers for iCCA. Indeed, recent data demonstrated that circRNAs are enriched in extracellular vesicles, including exosomes, compared to their linear counterparts.[37,38] The circular structure of circRNAs renders them more stable and resistant to degradation by exonucleases. Thus, pangenomic profiling of circRNA abundance is emerging in cancer, and several expression signatures have been reported, notably in HCC.[39] Our study provides the first report of circRNA expression in iCCA. The function of circRNA–TLINC remains to be explored, but several experimental data demonstrated that circRNAs may act as sponges for miRNA and RNA binding proteins. With respect to the TGF$\beta$ pathway, circRNA_010567 has been recently shown to promote TGF$\beta$-induced myocardial fibrosis by directly suppressing miR-141, which naturally targets TGF$\beta$.[40]

In conclusion, our study identifies novel TGF$\beta$ transcriptional target genes in iCCA, including an lncRNA that may represent a promising biomarker for iCCA.

*Acknowledgment:* We thank the core facilities of Biosit and Biogenouest (CRB Santé BB-0033-00056, GEH, $H^2P^2$, ImPACcell) and the French liver cancer biobanks network (BB-0033-00085), including Beaujon, Bordeaux, Mondor, Nantes, Paris-Sud, and Rennes biobanks. C.C. thanks K.A. Cole (Children's Hospital of Philadelphia) and S. Sugano (University of Tokyo) for providing the CASC15 DNA constructs; S. Dréano (Institut de génétique et développement de Rennes [IGDR]) for DNA sequencing; and C. Père for reporter sensor cell line analysis. We thank D. Gilot, M.D. Galibert (IGDR, Rennes), B. Fromenty (NuMeCan, Rennes), and S. Diederichs (German Cancer Research Center [DKFZ], Heidelberg) for helpful discussions.

## REFERENCES

1) Banales JM, Cardinale V, Carpino G, Marzioni M, Andersen JB, Invernizzi P, et al. Expert consensus document: cholangiocarcinoma: current knowledge and future perspectives consensus statement from the European Network for the Study of Cholangiocarcinoma (ENS-CCA). Nat Rev Gastroenterol Hepatol 2016;13:261-280.
2) Bridgewater J, Galle PR, Khan SA, Llovet JM, Park JW, Patel T, et al. Guidelines for the diagnosis and management of intrahepatic cholangiocarcinoma. J Hepatol 2014;60:1268-1289.
3) Moeini A, Sia D, Bardeesy N, Mazzaferro V, Llovet JM. Molecular pathogenesis and targeted therapies for intrahepatic cholangiocarcinoma. Clin Cancer Res 2016;22:291-300.
4) Sirica AE. The role of cancer-associated myofibroblasts in intrahepatic cholangiocarcinoma. Nat Rev Gastroenterol Hepatol 2011;9:44-54.
5) Rizvi S, Gores GJ. Pathogenesis, diagnosis, and management of cholangiocarcinoma. Gastroenterology 2013;145:1215-1229.
6) Sulpice L, Rayar M, Desille M, Turlin B, Fautrel A, Boucher E, et al. Molecular profiling of stroma identifies osteopontin as an independent predictor of poor prognosis in intrahepatic cholangiocarcinoma. Hepatology 2013;58:1992-2000.
7) Massague J. TGFbeta in cancer. Cell 2008;134:215-230.
8) Nieto MA, Huang RY, Jackson RA, Thiery JP. EMT: 2016. Cell 2016;166:21-45.
9) Ikushima H, Miyazono K. TGFbeta signalling: a complex web in cancer progression. Nat Rev Cancer 2010;10:415-424.
10) Massague J. TGFbeta signalling in context. Nat Rev Mol Cell Biol 2012;13:616-630.
11) Richards EJ, Zhang G, Li ZP, Permuth-Wey J, Challa S, Li Y, et al. Long non-coding RNAs (LncRNA) regulated by transforming growth factor (TGF) beta. LncRNA-HIT-mediated TGF-induced epithelial to mesenchymal transition in mammary epithelia. J Biol Chem 2016;291:22860.
12) Yuan JH, Yang F, Wang F, Ma JZ, Guo YJ, Tao QF, et al. A long noncoding RNA activated by TGF-beta promotes the invasion-metastasis cascade in hepatocellular carcinoma. Cancer Cell 2014;25:666-681.
13) Klingenberg M, Matsuda A, Diederichs S, Patel T. Non-coding RNA in hepatocellular carcinoma: mechanisms, biomarkers and therapeutic targets. J Hepatol 2017;67:603-618.
14) Prensner JR, Chinnaiyan AM. The emergence of lncRNAs in cancer biology. Cancer Discov 2011;1:391-407.
15) Allain C, Angenard G, Clement B, Coulouarn C. Integrative genomic analysis identifies the core transcriptional hallmarks of human hepatocellular carcinoma. Cancer Res 2016;76:6374-6381.

16) Coulouarn C, Corlu A, Glaise D, Guenon I, Thorgeirsson SS, Clement B. Hepatocyte-stellate cell cross-talk in the liver engenders a permissive inflammatory microenvironment that drives progression in hepatocellular carcinoma. Cancer Res 2012;72: 2533-2542.
17) Dubois-Pot-Schneider H, Fekir K, Coulouarn C, Glaise D, Aninat C, Jarnouen K, et al. Inflammatory cytokines promote the retrodifferentiation of tumor-derived hepatocyte-like cells to progenitor cells. Hepatology 2014;60:2077-2090.
18) Russell MR, Penikis A, Oldridge DA, Alvarez-Dominguez JR, McDaniel L, Diamond M, et al. CASC15-S is a tumor suppressor lncRNA at the 6p22 neuroblastoma susceptibility locus. Cancer Res 2015;75:3155-3166.
19) Lessard L, Liu M, Marzese DM, Wang H, Chong K, Kawas N, et al. The CASC15 long intergenic noncoding RNA locus is involved in melanoma progression and phenotype switching. J Invest Dermatol 2015;135:2464-2474.
20) Wu Y, Siadaty MS, Berens ME, Hampton GM, Theodorescu D. Overlapping gene expression profiles of cell migration and tumor invasion in human bladder cancer identify metallothionein 1E and nicotinamide N-methyltransferase as novel regulators of cell migration. Oncogene 2008;27:6679-6689.
21) Salzman J, Chen RE, Olsen MN, Wang PL, Brown PO. Cell-type specific features of circular RNA expression. PLoS Genet 2013;9:e1003777.
22) Giannelli G, Mikulits W, Dooley S, Fabregat I, Moustakas A, ten Dijke P, et al. The rationale for targeting TGF-beta in chronic liver diseases. Eur J Clin Invest 2016;46:349-361.
23) Yang W, Li Y, Song X, Xu J, Xie J. Genome-wide analysis of long noncoding RNA and mRNA co-expression profile in intrahepatic cholangiocarcinoma tissue by RNA sequencing. Oncotarget 2017;8:26591-26599.
24) Wang C, Mao ZP, Wang L, Wu GH, Zhang FH, Wang DY, et al. Long non-coding RNA MALAT1 promotes cholangiocarcinoma cell proliferation and invasion by activating PI3K/Akt pathway. Neoplasma 2017;64:725-731.
25) Coulouarn C, Factor VM, Thorgeirsson SS. Transforming growth factor-beta gene expression signature in mouse hepatocytes predicts clinical outcome in human cancer. Hepatology 2008;47:2059-2067.
26) Wang YY, Wu ZY, Wang GC, Liu K, Niu XB, Gu S, et al. LINC00312 inhibits the migration and invasion of bladder cancer cells by targeting miR-197-3p. Tumour Biol 2016;37:14553-14563.
27) Li M, Qiu M, Xu Y, Mao Q, Wang J, Dong G, et al. Differentially expressed protein-coding genes and long noncoding RNA in early-stage lung cancer. Tumour Biol 2015;36:9969-9978.
28) Waugh DJ, Wilson C. The interleukin-8 pathway in cancer. Clin Cancer Res 2008;14:6735-6741.
29) Liu Q, Li A, Tian Y, Wu JD, Liu Y, Li T, et al. The CXCL8-CXCR1/2 pathways in cancer. Cytokine Growth Factor Rev 2016;31:61-71.
30) Imamura K, Imamachi N, Akizuki G, Kumakura M, Kawaguchi A, Nagata K, et al. Long noncoding RNA NEAT1-dependent SFPQ relocation from promoter region to paraspeckle mediates IL8 expression upon immune stimuli. Mol Cell 2014;53:393-406.
31) Pandey RR, Mondal T, Mohammad F, Enroth S, Redrup L, Komorowski J, et al. Kcnq1ot1 antisense noncoding RNA mediates lineage-specific transcriptional silencing through chromatin-level regulation. Mol Cell 2008;32:232-246.
32) Hu G, Lou Z, Gupta M. The long non-coding RNA GAS5 cooperates with the eukaryotic translation initiation factor 4E to regulate c-Myc translation. PLoS One 2014;9:e107016.
33) Marquardt JU, Andersen JB, Thorgeirsson SS. Functional and genetic deconstruction of the cellular origin in liver cancer. Nat Rev Cancer 2015;15:653-667.
34) Tang X, Hou M, Ding Y, Li Z, Ren L, Gao G. Systematically profiling and annotating long intergenic non-coding RNAs in human embryonic stem cell. BMC Genomics 2013;14(Suppl. 5): S3.
35) Demoulin JB, Essaghir A. PDGF receptor signaling networks in normal and cancer cells. Cytokine Growth Factor Rev 2014;25: 273-283.
36) Steller EJ, Raats DA, Koster J, Rutten B, Govaert KM, Emmink BL, et al. PDGFRB promotes liver metastasis formation of mesenchymal-like colorectal tumor cells. Neoplasia 2013; 15:204-217.
37) Lasda E, Parker R. Circular RNAs co-precipitate with extracellular vesicles: a possible mechanism for circRNA clearance. PLoS One 2016;11:e0148407.
38) Li Y, Zheng Q, Bao C, Li S, Guo W, Zhao J, et al. Circular RNA is enriched and stable in exosomes: a promising biomarker for cancer diagnosis. Cell Res 2015;25:981-984.
39) Han D, Li J, Wang H, Su X, Hou J, Gu Y, et al. Circular RNA circMTO1 acts as the sponge of miR-9 to suppress hepatocellular carcinoma progression. Hepatology 2017;66:1151-1164.
40) Zhou B, Yu JW. A novel identified circular RNA, circRNA_010567, promotes myocardial fibrosis via suppressing miR-141 by targeting TGF-beta1. Biochem Biophys Res Commun 2017;487:769-775.

# Supporting Information

Additional Supporting Information may be found at onlinelibrary.wiley.com/doi/10.1002/hep4.1142/full.